R. M. Fonseca et al., Electrochemical Behavior of AISI 1020 Steel…, *Chem. Biochem. Eng. Q.*, **33** (2) 221–227 (2019)

221

Electrochemical Behavior of AISI 1020 Steel in Type C Commercial Gasolines

R. M. Fonseca,[*] R. A. D. Faria, J. C. da Silva Evangelista, L. H. O. Souza, B. A. Batista, R. B. Soares, and V. de Freitas Cunha Lins

Department of Chemical Engineering, Engineering School, Universidade Federal de Minas Gerais (UFMG), Belo Horizonte/MG, Brazil

In the present paper, the corrosion behavior of 1020 carbon steel in commercial gasoline-ethanol blends was investigated. The composition of each gasoline-ethanol blend was evaluated by infrared spectroscopy, and the ethanol content was determined by the ABNT 13992 reference method. Electrochemical Impedance Spectroscopy (EIS) and polarization methods were employed to evaluate corrosion resistance and penetration rates. Statistical analyses revealed that the gasoline's solution resistance governs the corrosion process, the RON (Research Octane Number) and MON (Motor Octane Number) numbers as well as the olefin content being more related to the corrosion rates. The polarization resistance had minor impact on the corrosion process.

Keywords:
ethanol-gasoline blends, carbon steel, corrosion, electrochemical impedance spectroscopy, polarization

Introduction

Fossil fuel vehicles figure amongst the greatest emitters of air pollutants in urban areas[1]. In line with global efforts to reduce CO_2 emissions and gaseous pollutants, as well as the search for renewable fuels, the automotive sector has experienced a growth in the use of biofuels over the past few years[2–4]. It is worth mentioning that the use of bioethanol in blends with gasoline is responsible for performance improvements on the automotive ignition system, reduction in pollutant emissions, increasing of the octane number[5], and fuel economy (1.5–5 %) when compared to pure gasoline[6]. Blends containing 20 % to 30 % of ethanol have common use due to low emission of pollutants[7].

The growing use of bioethanol for transport has resulted in discussions about possible corrosive mechanisms that could affect components and pose serious risks to user safety[8]. Despite recent developments on ethanol-compatible fuel systems (such as flex-fuel vehicles), gasoline and alcohol blends are customarily used in ordinary vehicles, which are then exposed to corrosion on some autoparts[4,9]. The corrosive mechanisms in these blends occurs due to the increased conductivity of ethanol in relation to gasoline[10], favoring electrochemical reactions; due to aging of biofuels producing acetic acid from ethanol[2]; or even due to the presence of trace elements with corrosive potential in fuel blends, such as aldehydes, peroxides, ketones, esters, among others[9]. The presence of water in the fuel can occur in situations of inadequate storage of the fuel, given the hygroscopic nature of ethanol, leading to phase separation.

As one of the largest producers and consumers of ethanol around the globe, Brazil has adopted regulations regarding the maximum ethanol content in commercial gasoline[11]. The Brazilian National Agency of Petroleum, Natural Gas and Biofuels (ANP, Brazilian Ministry of Mines and Energy), regulates the maximum ethanol content in commercial gasoline as 27 % by volume[12]. Adulteration of gasoline by surpassing the legal ethanol content is the biggest cause of noncompliance in gasoline samples in Brazil[13].

This work aimed to determine the corrosion behavior of SAE 1020 carbon steel in commercial gasoline-ethanol blends available in Brazil. The investigations were carried out by determining the chemical composition of fuel samples, and using Electrochemical Impedance Spectroscopy (EIS) and polarization methods to evaluate the corrosion behavior of steel in gasoline.

*Corresponding author: e-mail address: rafaelamfons@gmail.com

Material and methods

Materials and specimens

The corrosion tests were performed on SAE (Society of Automotive Engineers) 1020 carbon steel samples. Specimens of 1 cm x 1 cm were welded to a copper wire in order to generate electrical contact. The set was embedded in epoxy resin (Akasel – Aka-Cure) to expose only the metal surface to the gasoline medium.

The surface of the working electrode was mechanically polished using a standard polishing machine with silicon carbide papers with 500, 600, 800 and 1200 grits prior to the electrochemical tests. The electrodes were then cleaned with distilled water, and dried in blowing air.

The corrosion medium used in this study was commercial gasoline purchased from three automotive fuel retail brands available in Brazil (herein named as "A", "B" and "C"), encompassing nine different gas stations (three from each brand) in Belo Horizonte city, Brazil. Accordingly, the samples regarding each fuel retail brand and the respective gas station were named as follows: A1, A2, A3, B1, B2, B3, C1, C2, and C3.

Determination of anhydrous ethanol in gasoline

The anhydrous ethanol content in gasoline was determined by the reference method according to the ABNT-NBR13992[14] standard. The ethanol content (EC, %v/v) was calculated according to Eq. (1), in which "*A*" is the final volume of the aqueous phase (in milliliters).

$$EC = (A - 50) \cdot 2 + 1 \tag{1}$$

Gasoline composition

In this work, the gasoline composition was assessed with respect to the following parameters: Research Octane Number (RON), Motor Octane Number (MON), Antiknock Index (AKI, estimated as (MON+RON)/2) and the percentages (in %v/v) of olefins, saturated hydrocarbons, aromatics, and benzene (ASTM D6277)[16]. These parameters were determined using a Petrospec portable analyzer, model GS 1000 PLUS with spectral range of 400–4000 cm^{-1}.

EIS measurements

According to Jafari *et al.*[16], the use of two electrodes for EIS measurements in gasoline is considered optimum, due to its high electrical resistance. The electrochemical studies were carried out using a two-electrode glass cell with a capacity of 100 mL. The gasoline samples were used as electrolytes,

and no supporting electrolyte was added to the fuel solution in order to avoid the interference of other possible corrosive interferers.

EIS measurement was performed using a Princeton Applied Research model Versa Stat 3 potentiostat controlled with Versa Studio software, with the SAE 1020 steel specimens as the working electrode, and platinum as auxiliary electrode. The distance between working and auxiliary/reference electrodes was kept to a minimum, in order to achieve more reliable results. Impedance diagrams were recorded in a frequency range from 100 to 0.007 Hz, and an amplitude of 20 mV within the range of corrosion potential (E_{corr}) was applied. The tests were carried out in triplicate and, afterwards, EIS data were modelled to an electrical equivalent circuit by fitting with the Zview2.0 software.

Polarization measurements

Polarization tests were performed using the Autolab PGSTAT 100N potentiostat connected to an electrochemical cell consisting of the carbon steel as working electrode, a platinum counter-electrode, and an Ag/AgCl reference electrode. The open circuit potential (OCP) was monitored for 900 s before polarization. The potential sweep was performed at a scan rate of 1.0 mV s^{-1}. The polarization range was ± 250 mV in relation to the stabilized OCP. The corrosion rates were estimated from Tafel extrapolation according to Eq. (2) and Eq. (3) as the metal weight loss rate (*r*) and the metal penetration rate (*r'*). In the equations, "*M*" is the metal molar mass (55.76 g mol^{-1}), "*j*" is the corrosion current density (A cm^{-2}), "*n*" is the number of exchanged electrons (*n* = 2), "*F*" is the Faraday constant (96,500 C mol^{-1}), and "*ρ*" is the metal density (0.00786 g mm^{-3}).

$$r = 8.64 \cdot 10^{8} \frac{Mj}{nF} \tag{2}$$

$$r' = 3.65 \cdot 10^{-4} \frac{r}{\rho} \tag{3}$$

Results and discussion

Gasoline composition

The anhydrous ethanol content in each gasoline sample is shown in Fig. 1. All samples indicated conformity with the previously mentioned regulation[12], and their average anhydrous ethanol content was equal to 27 % v/v at a confidence level of 95 %.

Table 1 shows the results in terms of compositions for the various samples. Apart from the benzene content, where all samples failed the specified values, the regulatory limits were fulfilled in every

Table 1 – *Composition of gasoline from different automotive fuel retail brands*

| Parameter	Reference value[20] (%v/v)	Sample (%v/v)								
		A1	A2	A3	B1	B2	B3	C1	C2	C3
RON	Not specified	100.0	100.5	100.0	100.0	99.8	100.2	100.5	96.9	97.0
MON (min)	82.0	102.3	108.1	105.9	99.3	99.4	102.9	92.2	91.1	91.5
AKI (min)	87.0	101.2	104.3	103.0	99.7	99.6	101.6	96.3	94.0	94.3
Olefins (max)	25.0	0.0	0.0	0.0	0.0	0.0	0.0	5.2	0.7	0.7
Saturated hydrocarbons	Not specified	62.3	64.5	63.9	60.3	60.4	60.1	50.6	62.8	63.0
Aromatics (max)	35.0	4.5	1.8	2.5	6.1	5.7	4.1	9.9	5.6	5.6
Benzene (max)	1.00	2.14	2.60	2.46	1.86	1.88	2.23	1.41	1.13	1.19
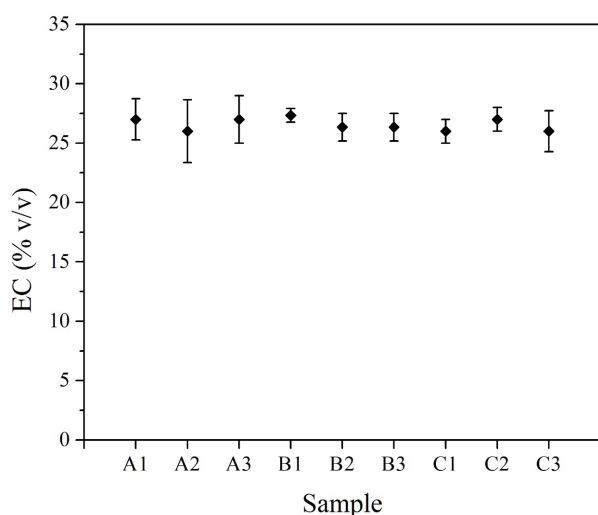
Fig. 1 – *Results of anhydrous ethanol content using a 95 % confidence interval for the mean measurements*

characteristic. For the specimen C1, unusual results were found for the olefins, as well as the saturated hydrocarbons contents. Amongst all samples, C1 showed the highest olefins and aromatic content in addition to the lowest saturated hydrocarbon content.

Olefins (carbon compounds with two or more double bonds) are suggested to enhance the gasoline reactivity in combustion processes, the octane number, and the anti-knock performance[17]. It has been reported that a high content of olefins in fuels may increase ozone emissions and form gum deposits in automotive fuel systems[17,18]. Unlike the olefins, saturated hydrocarbons figure as the most stable constituents of gasoline[18].

EIS measurements

Fig. 2 represents the Bode plots for the SAE 1020 carbon steel in gasoline for each of the three automotive fuel retail brands evaluated.

Based on the Bode plots, an electrical equivalent circuit was proposed to represent the corrosion process of the SAE 1020 carbon steel in commercial gasoline, as shown in Fig. 2. The proposed equivalent circuit was also used by Jafari *et al.*[16] and Deyab[3], and consisted of a solution resistance (R_S), a polarization resistance (R_p), and a constant phase element (CPE), instead of an ideal capacitor, in order to take into account surface heterogeneities[19]. EIS data was fitted to the proposed model. The simulated parameters are shown in Table 2.

The high impedance observed in all the samples was due to the high resistivity of the gasoline, which hindered the development of the electrical double layer on the interface with the steel electrode[20].

The solution resistance (Fig. 3) seemed to vary considerably inside each test group (automotive fuel retail brand). In general, brand C presented higher polarization resistances in comparison to the other groups. Brand B seemed to present the lowest variation amongst samples. As expected from the composition results, sample C1 presented the lowest solution resistance, which may be attributed to the higher aromatic content. The lowest electrochemical resistance of aromatic components was due to a negative charge density induced by the aromatic ring[21] that allowed for increased conductivities. The R_p results showed higher variation, in general, when compared to the R_S results, and samples C2 and C3 presented much higher R_p values, comparatively. This again may be related to low RON and MON values. Despite the samples differing with respect to R_S and R_p values, there was insufficient statistical evidence to conclude that the mean values for both parameters in each fuel retail brand differed at the 0.05 level of significance.

Samples C2 and C3 presented the lowest values for RON and MON numbers. These parameters
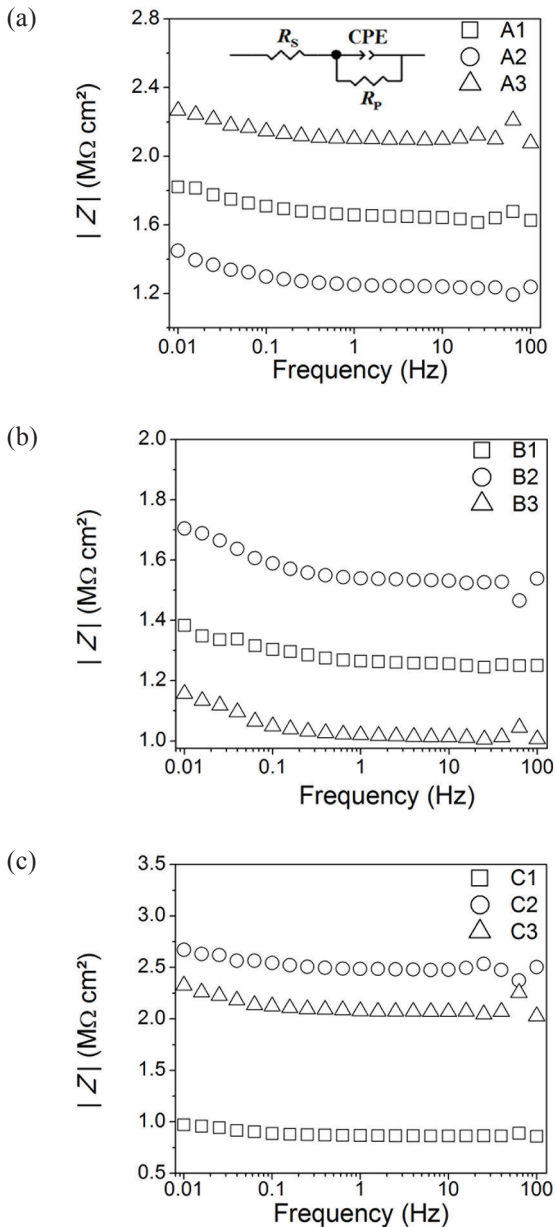
(a)

(b)

(c)

Fig. 2 – *Bode diagrams for 1020 carbon steel in commercial gasoline from automotive fuel retail brands A (a), B (b) and C (c)*
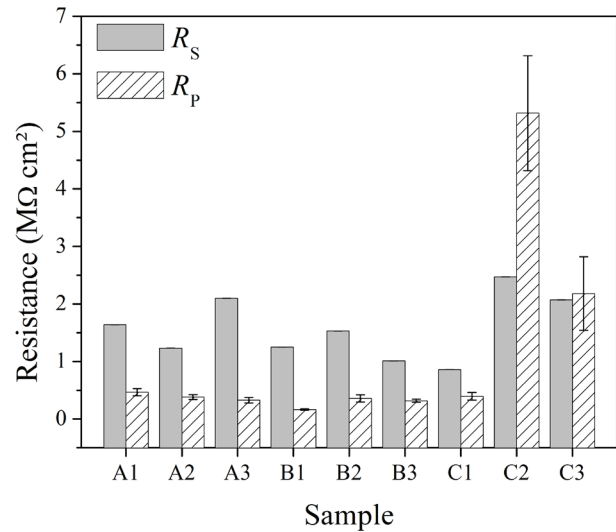

Fig. 3 – *Calculated R_S and R_P for the different samples*

indicate the fuel's tendency to auto-ignite, and are influenced by reactive components in the fuel, such as ethanol content[5,17,22]. Accordingly, since ethanol has been used also as an important modifier of octane number in gasoline, variations regarding MON and RON numbers could be related to the ethanol content in the gasoline samples, which is an important component responsible for gasoline corrosiveness. According to Matějovský *et al.*[21] the presence of ethanol in the fuel composition can increase the conductivity of the solution and alter its compatibility with metallic materials kept in contact with the gasoline in vehicle fuel system components. These authors have mentioned that the presence of bioethanol in ethanol-gasoline blends, for instance, leads to an increase in oxidation susceptibility of the fuel, which causes the formation of corrosive byproducts. Since the ethanol content in the examined samples did not significantly vary individually nor among the brand groups, the slight decrease in the octane number parameters in samples C2 and C3 might have arisen from the influence of other fuel

Table 2 – *Estimated impedance parameters*

Sample	R_S (MΩ cm^2)	R_P (MΩ cm^2)	CPE ($\mu\Omega^{-1}$ cm^{-2} s^n)	χ^2
A1	1.6363 ± 0.0023	0.4646 ± 0.0632	11.898 ± 0.449	0.0007
A2	1.2318 ± 0.0024	0.3805 ± 0.0436	13.675 ± 0.412	0.0007
A3	2.0958 ± 0.0042	0.3276 ± 0.0483	16.465 ± 1.668	0.0029
B1	1.2516 ± 0.0020	0.1630 ± 0.0108	14.835 ± 0.879	0.0010
B2	1.5273 ± 0.0015	0.3560 ± 0.0632	13.766 ± 0.422	0.0005
B3	1.0099 ± 0.0015	0.3169 ± 0.0252	19.513 ± 0.856	0.0012
C1	0.8594 ± 0.0016	0.3955 ± 0.0649	26.428 ± 1.467	0.0012
C2	2.4718 ± 0.0042	5.3167 ± 1.0124	13.511 ± 0.752	0.0019
C3	2.0681 ± 0.0029	2.1792 ± 0.5441	12.940 ± 0.521	0.0012

components, like olefins, which are known to impact MON and RON values. Thus, the high solution resistance presented by these two samples may be attributed to the fuel's lower reactivity due to small-
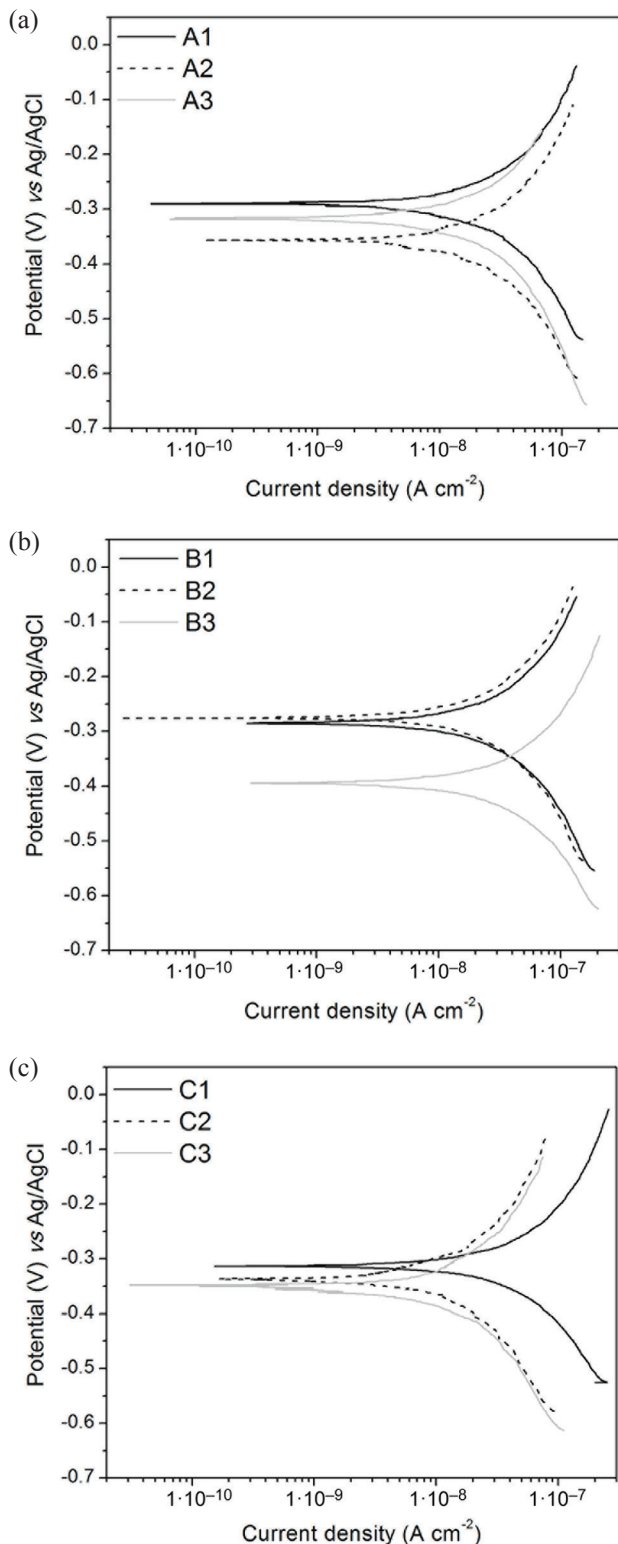

Fig. 4 – *Polarization curves for 1020 carbon steel in commercial gasoline from automotive fuel retail brands A (a), B (b), and C (c)*

Table 3 – *Calculated penetration and corrosion rates of gasoline from different automotive fuel retail brands*

Sample	Penetration rate, r' (mm year^{-1})	Corrosion rate, r (g m^{-2} day^{-1})
A1	$1.46 \cdot 10^{-4}$	$3.15 \cdot 10^{-3}$
A2	$8.45 \cdot 10^{-4}$	$1.82 \cdot 10^{-2}$
A3	$2.39 \cdot 10^{-4}$	$5.14 \cdot 10^{-3}$
B1	$3.60 \cdot 10^{-4}$	$7.76 \cdot 10^{-3}$
B2	$2.47 \cdot 10^{-4}$	$5.33 \cdot 10^{-3}$
B3	$7.88 \cdot 10^{-4}$	$1.70 \cdot 10^{-2}$
C1	$8.18 \cdot 10^{-4}$	$1.76 \cdot 10^{-2}$
C2	$9.08 \cdot 10^{-5}$	$1.96 \cdot 10^{-3}$
C3	$9.58 \cdot 10^{-5}$	$2.06 \cdot 10^{-3}$

er RON and MON numbers. In addition, the C2 and C3 samples showed olefin contents lower than C1 sample, and this fact could have contributed to the lowest polarization resistance value of C1 sample.

Polarization measurements

Fig. 4 shows the polarization curves obtained for SAE 1020 carbon steel in gasoline for each of the three automotive fuel retail brands evaluated.

Table 3 shows the calculated penetration and corrosion rates for each of the tested samples. All calculated rates agreed with other literature results[3,9].

Sample C1 was amongst those with the most significant relation between the solution resistance and the corrosion rate. Samples C2 and C3 presented lower corrosion rates as a direct relation to their high solution and polarization resistances.

Carrying out further investigation on the influence of these two resistances on the corrosion process, a linear regression analysis was proposed in order to minimize the sum of square errors in the model. The model was expressed according to the following equation:

$$Y = \beta_0 + \beta_1 x_1 + \beta_2 x_2 \tag{4}$$

where Y is the response variable, β_i are the regression coefficients, and x_i are the levels of the independent variables.

The penetration rate was set as the dependent variable or response, Y. The two independent variables were $1/R_S$ (x_1) and $1/R_P$ (x_2). The results are summarized in Table 4.

On the basis of the data obtained, an equation was generated to establish the correlation between the independent variables and the dependent variable. The model was expressed as follows:

$$Y = -3.84 \cdot 10^{-4} + 1.17 \cdot 10^{3} x_1 - 16.80 x_2 \qquad (5)$$

Analysis of variance in Table 4 showed that factor $1/R_S$, unlike factor $1/R_p$, had a significant effect on the average penetration rate, at a probability level of $\alpha = 0.05$. Therefore, the solution resistance mainly governed the corrosion process, which corroborates the previous discussions, since R_S is a consequence of solution composition. Thus, the slight variations in the samples' composition (mainly towards the ethanol content) reflected equally on low corrosiveness variations of each sample as a consequence of quality conformity of the fuel brands A, B, and C in relation to the parameters preconized in the specific regulation[20] (except for the benzene concentration).

Given the significant effect of the solution resistance on the corrosion process, the model described in Eq. (6) was proposed to represent the penetration rate in terms of the inverse of the solution resistance.

$$Y = \beta_0 + \beta_1 x_3 \qquad (6)$$

where Y is the dependent variable, set as $\ln(r')$; β_i are the regression coefficients; and x_3 is independent variable, set as $\ln(1/R_S)$.

The fitting results are summarized in Table 5. The equation, generated by the fitting, which establishes the correlation between the corrosion rate and the solution resistance, is as follows:

$$\ln(r') = 23.98 + 2.26 \ln\left(\frac{1}{R_S}\right) \qquad (7)$$

Analysis of variance in Table 5 showed that the solution resistance was significant at the probability level of $\alpha = 0.05$. Increasing the solution resistance should have caused a decrease in the corrosion rate. The high coefficient of determination, $R^2 = 0.81$, and

$F = 30.26$ ($> F_{1,7,0.05} = 5.59$) verified that the model was adequate at a probability level of $\alpha = 0.05$. The normal probability plot showed no departure from the normality assumption, since the points fell alongside the straight line, as in Fig. 5a. The assumption of constant variance also appeared reasonable, since the residual vs fit plot showed random points distribution (Fig. 5b).
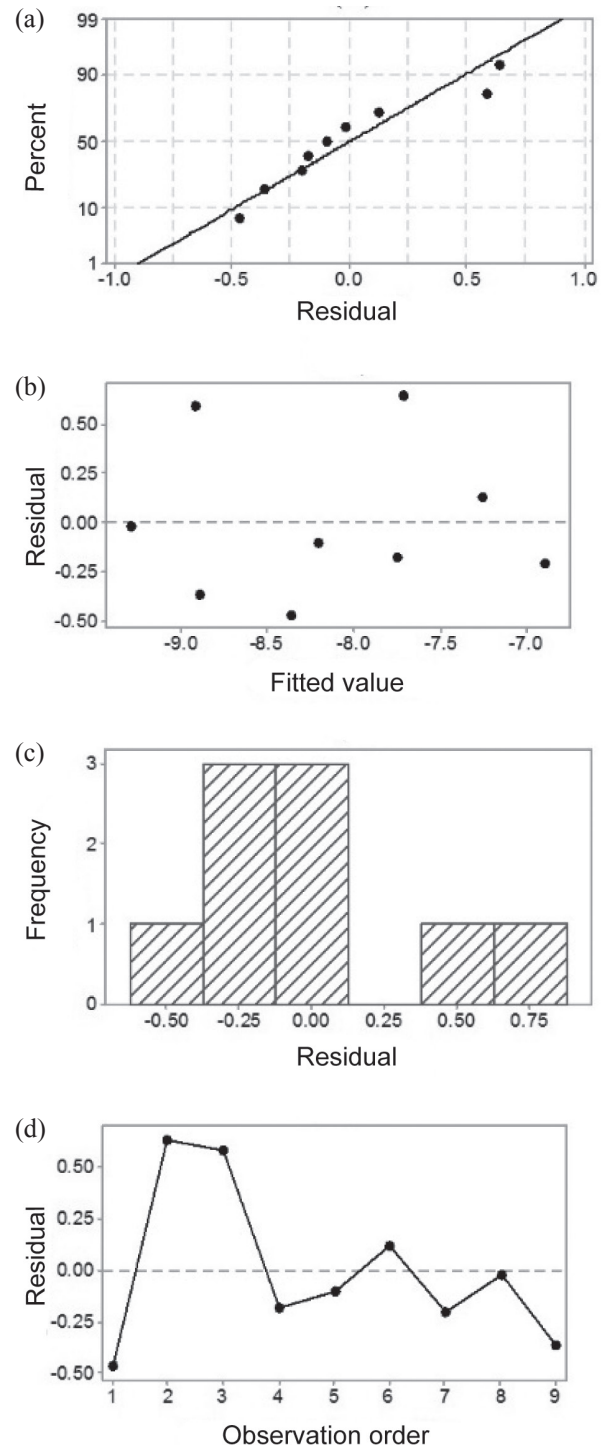

Fig. 5 – *Residual plots for the proposed model*

Table 4 – *Results of regression analysis for the penetration rate in response to the inverse of the solution and polarization resistances*

Term	Coefficient	t-value	p-value
intercept	$-3.84 \cdot 10^{-4}$	-2.12	0.078
x_1	$1.17 \cdot 10^{3}$	4.33	0.005
x_2	-16.80	-0.42	0.688

Table 5 – *Results of regression analysis for the model proposed in Eq. 6*

Term	Coefficient	t-value	p-value
intercept	23.98	4.10	0.005
x_1	2.26	5.50	0.001

Conclusions

Based on the composition results, the anhydrous ethanol content was very similar for all tested samples (approximately 27 %v/v). Furthermore, apart from the benzene content, all the fuel samples presented composition in agreement with the limits established in the appropriate regulation.

Amongst all the brands, group C was the one with the higher polarization resistances. Samples C2 and C3 possessed the higher R_p values in the group, which may be associated with their lower RON and MON values, comparatively. On the other hand, C1 presented higher aromatic content, possibly due to the negative charge density arising from the double bonds of the aromatic rings.

Statistically, R_S was the most important parameter in the corrosiveness of the samples. However, the small variations observed in the composition of the samples (mainly with respect to ethanol content) reflected low variations of their corrosion rates.

References

1. *Thakur, A. K., Kaviti, A. K., Mehra, R., Mer, K. K. S.,* Progress in performance analysis of ethanol-gasoline blends on SI engine, Renew. Sustain. Energy Rev. **69** (2017) 324.
   doi: https://doi.org/10.1016/j.rser.2016.11.056

2. *Abel, J., Virtanen, S.,* Corrosion of martensitic stainless steel in ethanol-containing gasoline: Influence of contamination by chloride, H_2O and acetic acid, Corros. Sci. **98** (2015) 318.
   doi: https://doi.org/10.1016/j.corsci.2015.05.027

3. *Deyab, M. A.,* Adsorption and inhibition effect of Ascorbyl palmitate on corrosion of carbon steel in ethanol blended gasoline containing water as a contaminant, Corros. Sci. **80** (2014) 359.
   doi: https://doi.org/10.1016/j.corsci.2013.11.056

4. *Park, I.-J., Nam, T.-H., Kim, J.-H., Kim, J.-G.,* Evaluation of corrosion characteristics of aluminum alloys in the bio-ethanol gasoline blended fuel by 2-electrode electrochemical impedance spectroscopy, Fuel **126** (2014) 26.
   doi: https://doi.org/10.1016/j.fuel.2014.02.030

5. *Niven, R. K.,* Ethanol in gasoline: Environmental impacts and sustainability review article, Renew. Sustain. Energy Rev. **9** (2005) 535.

6. URL: http://docplayer.net/21255654-Fuel-economy-study-comparing-performance-and-cost-of-various-ethanol-blends-and-standard-unleaded-gasoline-american-coalition-for-ethanol.html (02.1.2019.)

7. *Chen, R.-H., Chiang, L.-B., Chen, C.-N., Lin, T.-H.,* Cold-start emissions of an SI engine using ethanol-gasoline blended fuel, Appl. Therm. Eng. **31** (2011) 1463.
   doi: https://doi.org/10.1016/j.applthermaleng.2011.01.021

8. *Park, I. J., Yoo, Y. H., Kim, J. G., Kwak, D. H., Ji, W. S.,* Corrosion characteristics of aluminum alloy in bio-ethanol blended gasoline fuel: Part 2. The effects of dissolved oxygen in the fuel, Fuel **90** (2011) 633.
   doi: https://doi.org/10.1016/j.fuel.2010.09.049

9. *Baena, L. M., Gómez, M., Calderón, J. A.,* Aggressiveness of a 20 % bioethanol–80 % gasoline mixture on autoparts: I behavior of metallic materials and evaluation of their electrochemical properties, Fuel **95** (2012) 320.
   doi: https://doi.org/10.1016/j.fuel.2011.12.002

10. *Thomson, J. K., Pawel, S. J., Wilson, D. F.,* Susceptibility of aluminum alloys to corrosion in simulated fuel blends containing ethanol, Fuel **111** (2013) 592.
    doi: https://doi.org/10.1016/j.fuel.2013.04.047

11. *Fortunato, F. M., Vieira, A. L., Neto, J. A. G., Donati, G. L., Jones, B. T.,* Expanding the potentialities of standard dilution analysis: Determination of ethanol in gasoline by Raman spectroscopy, Microchem. J. **133** (2017) 76.
    doi: https://doi.org/10.1016/j.microc.2017.03.015

12. MAPA. Portaria nº 75. Fixa, o percentual obrigatório de adição de etanol anidro combustível à gasolina. Diário Oficial da União (2015).

13. *Avila, L. M., Santos, A. P. F., Mattos, D. I. M., Souza, C. G., Andrade, D. F., D'Avila, L. A.,* Determination of ethanol in gasoline by high-performance liquid chromatography, Fuel **212** (2018) 236.
    doi: https://doi.org/10.1016/j.fuel.2017.10.039

14. ABNT, Gasolina automotiva – Determinação do teor de álcool etílico anidro combustível (AEAC) – NBR 13992 (1997).

15. ASTM® D6277-07, 2007. Standard Test Method for Determination of Benzene in Spark-Ignition Engine Fuels Using Mid Infrared Spectroscopy. ASTM® International.
    doi: https://doi.org/10.1520/d6277-07

16. *Jafari, H., Idris, M. H., Ourdjini, A., Rahimi, H., Ghobadian, B.,* EIS study of corrosion behavior of metallic materials in ethanol blended gasoline containing water as a contaminant, Fuel **90** (2011) 1181.
    doi: https://doi.org/10.1016/j.fuel.2010.12.010

17. *Hajbabaei, M., Karavalakis, G., Miller, J. W., Villela, M., Xu, K. H., Durbin, T. D.,* Impact of olefin content on criteria and toxic emissions from modern gasoline vehicles, Fuel **107** (2013) 671.
    doi: https://doi.org/10.1016/j.fuel.2012.12.031

18. *Pereira, R. C., Pasa, V. M. D.,* Effect of mono-olefins and diolefins on the stability of automotive gasoline, Fuel **85** (2006) 1860.
    doi: https://doi.org/10.1016/j.fuel.2006.01.022

19. *Popova, A., Sokolova, E., Raicheva, S., Christov, M.,* AC and DC study of the temperature effect on mild steel corrosion in acid media in the presence of benzimidazole derivatives, Corros. Sci. **45** (2003) 33.
    doi: https://doi.org/10.1016/s0010-938x(02)00072-0

20. Agência Nacional do Petróleo (ANP) nº 40/2013 – Especificação da gasolina de uso automotivo. URL:www.anp.gov.br (30.11.2018.)

21. *Matějovský, L., Macák, J., Pospíšil, M., Baroš P., Staš, M., Krausová, A.,* Study of corrosion of metallic materials in ethanol–gasoline blends: Application of electrochemical methods, Energy & Fuels **31** (2017) 10880.
    doi: https://doi.org/10.1021/acs.energyfuels.7b01682

22. *Badra, J., AlRamadan, A. S., Sarathy, S. M.,* Optimization of the octane response of gasoline/ethanol blends, Appl. Energy **203** (2017) 778.
    doi: https://doi.org/10.1016/j.apenergy.2017.06.084